Eisaku Suwa, Yuichi Tsujiura, Fumiya Kurokawa, Hirotaka Hida and Isaku Kanno*

Fabrication of High-Efficiency Piezoelectric Energy Harvesters of Epitaxial $Pb(Zr,Ti)O_3$ Thin Films by Laser Lift-off

Abstract: We fabricated piezoelectric vibration energy harvesters of *c*-axis-oriented epitaxial $Pb(Zr,Ti)O_3$ (PZT) thin films on stainless steel (SS304) cantilevers in an effort to improve their power-generation efficiency and toughness. Using radio-frequency magnetron sputtering, we deposited the epitaxial PZT thin films on the MgO substrates, and then transferred the PZT films onto microfabricated SS304 cantilevers using laser lift-off (LLO). LLO did not degrade the transferred epitaxial PZT thin films, which exhibited a high piezoelectric coefficient ($e_{31,f} = -4.8$ C/m^2) and a low relative dielectric constant ($\varepsilon_r = 340$), comparable to those of the original PZT thin film on MgO. At a resonance frequency of 143 Hz, the energy harvesters generated large output power of 1.8 μW at an acceleration of 1.0 m/s^2, and the output power reached a maximum of 49 μW at an acceleration of 7.5 m/s^2.

Keywords: piezoelectric energy harvester, epitaxial PZT, laser lift-off

DOI 10.1515/ehs-2014-0046

Introduction

Recently, piezoelectric vibration energy harvesters (PVEHs) have attracted attention as promising power sources for battery-free wireless sensor nodes. Compared with other types of vibration energy harvesters, such as electrostatic or electromagnetic generators, PVEHs are advantageous because they are small, simple, and have high energy efficiency because piezoelectric materials have excellent electromechanical transfer characteristics.

Conventional MEMS PVEHs are composed of PZT-deposited silicon (Si) cantilevers. To maximize the output power of a PVEH, its resonance frequency should be adjusted to the peak frequencies of environmental vibrations, typically less than 200 Hz (Kim, Priya, and Kanno 2012). Thus, thinner cantilevers with large tip mass are preferable. However, thin Si cantilevers are brittle, making them break easily under large vibrations. One way to improve the toughness of PVEHs is to use metal cantilevers (Cao, Zhang, and Kuwano 2012; Kanda et al. 2009; Lin and Wu 2013; Tsujiura, Adachi, and Kanno 2012; Tsujiura et al. 2013). The fracture toughness of austenitic stainless steel (SS304) is more than 100 MPam$^{1/2}$, a hundred times larger than that of Si (Ericson, Johansson, and Schweitz 1988; Murase et al. 1993). Metal cantilevers can be reduced in thickness to less than a few tens of micrometers while maintaining sufficient toughness. These properties of metal cantilevers make it easy to lower their resonance frequency.

On the other hand, the most important research in MEMS PVEHs is improving power-generation efficiency. Piezoelectric materials with high piezoelectric coefficients and low relative dielectric constants are required to enhance power generation efficiency (Yeager and Trolier-McKinstry 2012). Conventional MEMS PVEHs are usually made of $Pb(Zr,Ti)O_3$ (PZT) thin films with compositions near the morphotropic phase boundary. PZT thin films on Si substrates exhibit large piezoelectric coefficients $e_{31,f}$ (−8 to −10 C/m^2), but their relative dielectric constant is ~1,000 (Tomioka et al. 2012; Trolier-Mckinstry and Muralt 2004). On the other hand, *c*-axis-oriented epitaxial PZT thin films have not only high piezoelectric coefficients but also low dielectric coefficients (Yeager and Trolier-McKinstry 2012). However, epitaxial PZT thin films are usually deposited only on epitaxial substrates such as MgO and $SrTiO_3$ or on Si substrates with multiple buffer layers (Isarakorn et al. 2010; Kanno, Fujii, and Takayama 1997; Yin et al. 2012; Yokoyama et al. 2005), making it difficult to microfabricate epitaxial PZT thin films including the substrate by conventional methods.

***Corresponding author: Isaku Kanno,** Department of Mechanical Engineering, Kobe University, Kobe 657–8501, Japan, E-mail: kanno@mech.kobe-u.ac.jp
Eisaku Suwa: E-mail: eisaku.suwa@stu.kobe-u.ac.jp, **Yuichi Tsujiura:** E-mail: tsujiura@stu.kobe-u.ac.jp, **Fumiya Kurokawa:** E-mail: fumiya.kurokawa@stu.kobe-u.ac.jp, **Hirotaka Hida:** E-mail: hida@mech.kobe-u.ac.jp, Department of Mechanical Engineering, Kobe University, Kobe 657–8501, Japan

Morimoto et al. fabricated PVEHs of epitaxial PZT thin films, transferred from MgO substrates to stainless cantilevers, which had better power generation performance than PVEHs of polycrystalline PZT thin films (Morimoto et al. 2010). They fabricated the epitaxial PZT thin film on a MgO substrate; after bonding the PZT and stainless cantilever, they wet etched the substrate. However, this method often overetches the thick MgO substrate, degrading or damaging the PZT film. An alternative method is laser lift-off (LLO), a dry process (Tsakalakos and Sands 2000; Tsakalalos et al. 2003). In LLO, an excimer laser irradiates the PZT thin film from the backside of the MgO substrate, allowing the epitaxial PZT thin films to be removed from the MgO. Energy harvesters fabricated by LLO are reported by Do et al. (2012; 2013); Lee et al. (2010); Park et al. (2014). However, these energy harvesters were made of non-epitaxial PZT thin films transferred to flexible substrates.

In this study, we fabricated high-efficiency energy harvesters of epitaxial PZT thin films on stainless steel cantilevers. Using LLO, we transferred *c*-axis-oriented epitaxial PZT thin films to microfabricated stainless steel cantilevers, and then evaluated the power-generation efficiency of the harvesters.

Device fabrication

We fabricated PVEHs of epitaxial PZT thin films transferred to stainless steel (SS304) cantilevers. SS304 cantilevers (10×10 mm^2, 30 μm thickness) with built-in tip mass were prepared by two-step spray etching (Tsujiura, Adachi, and Kanno 2012; Tsujiura et al. 2013). Figure 1 shows the PVEH fabrication process. The *c*-axis-oriented epitaxial PZT thin films were grown on (001) single-crystal MgO substrates by radio-frequency (rf) magnetron sputtering (Figure 1(a)). The sputtering conditions of the epitaxial PZT thin films were reported in our previous study (Kanno, Fujii, and Takayama 1997). After PZT deposition, we deposited Cr layer as electrodes (Figure 1(b)).

The PZT thin films were transferred to the SS304 cantilevers using LLO. Prior to LLO, we bonded the PZT/MgO substrates to the SS304 cantilevers with epoxy (Huntsman, Araldite Rapid) so the Cr electrodes faced the SS304 cantilever (Figure 1(c)). Then, a KrF excimer laser ($\lambda = 248$ nm) irradiated the backside of the MgO substrates (Figure 1(d)). Because the photon energy of KrF (5 eV) is lower than the band gap of MgO (8 eV) and higher than that of PZT (3.4 eV), the KrF beam transmits through MgO and is absorbed at the PZT/MgO interface (Do et al. 2012; 2013; Lee et al. 2010; Pandey et al. 2005; Park et al. 2014; Tsakalakos and Sands 2000; Tsakalaos et al. 2003). The absorbed photon energy separates the PZT thin film from the MgO substrate (Figure 1(e)). The laser pulses were scanned over the whole PZT thin films to eventually remove the MgO substrate from the PZT-bonded SS304 cantilevers.

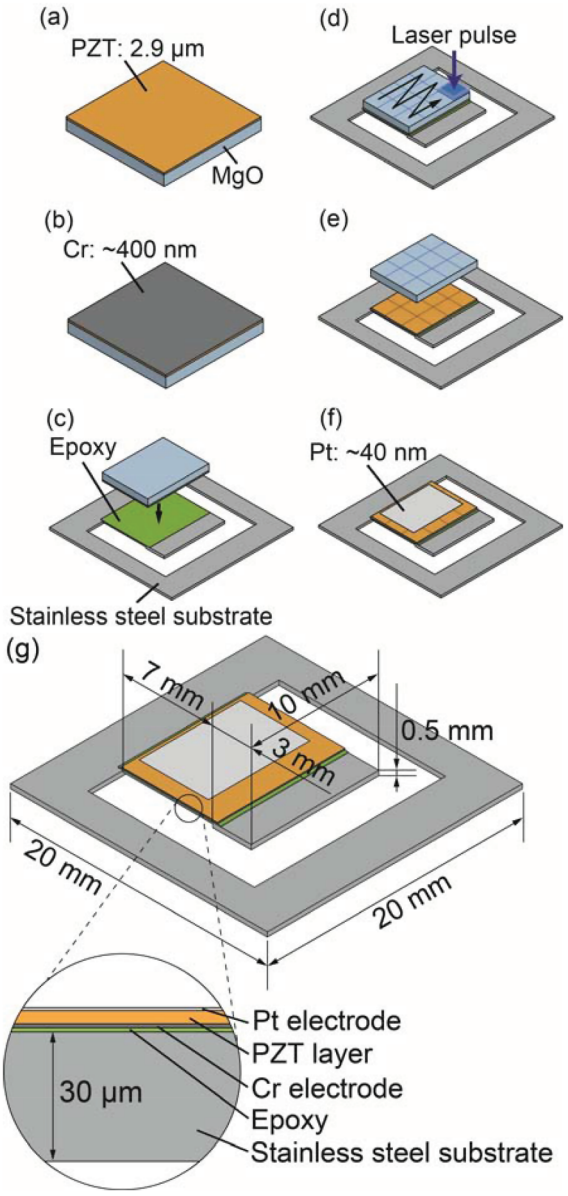

Figure 1: Fabrication process of PVEHs of *c*-axis-oriented epitaxial PZT thin films: (a) Deposition of PZT thin film on single-crystal MgO by rf magnetron sputtering, (b) deposition of Cr electrode, (c) bonding with microfabricated SS304 cantilever, (d) excimer laser irradiation from the backside of MgO, (e) removal of MgO, (f) deposition of Pt electrode, (g) schematic of a PVEH of a *c*-axis-oriented epitaxial PZT thin film.

Table 1 shows the LLO conditions. Figure 2 shows an optical image of the transferred epitaxial PZT thin film.

Table 1: Conditions for laser lift-off.

Gas	KrF
Wavelength [nm]	248
Energy density [mJ/mm^2]	25~30
Irradiated area per one shot [mm × mm]	2.3 × 2.3–2.5 × 2.5
Feed speed [mm]	2.2

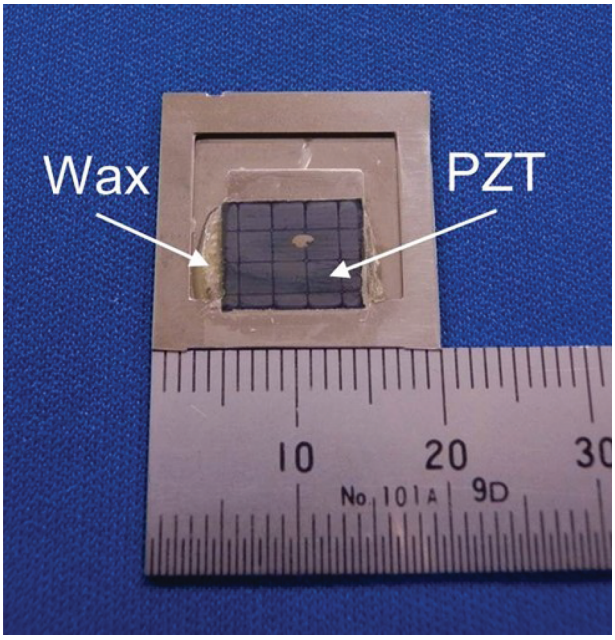

Figure 2: Photograph of piezoelectric energy harvester after LLO.

The lattice-like surface pattern on the transferred PZT corresponds to the single-shot area of the laser pulses. Because the cantilevers were as thin as 30 μm, we fixed their backsides with electron wax to prevent the laser shots from deforming them. By optimizing the laser energy density to 25–30 mJ/mm^2, we transferred the *c*-axis-oriented PZT thin films to the SS304 cantilevers. After transferring the PZT thin films, we deposited Pt surface electrodes by rf magnetron sputtering, completing the PVEHs (Figure 1(f)).

Piezoelectric properties and crystal structure of transferred PZT thin films

After transferring the epitaxial PZT thin films, we evaluated their electrical properties. We found their relative dielectric constant and dielectric loss to be 340 and 3.9%, respectively. These values are typical for *c*-axis-oriented epitaxial PZT thin films on Pt/MgO substrates (Kanno, Fujii, and Takayama 1997).

We also measured the piezoelectric properties of the transferred PZT thin films from the converse piezoelectric effect of the transferred PZT/SS304 unimorph cantilevers. Because the electrodes and epoxy layers were sufficiently thin, we ignored their effect. The piezoelectric coefficient $e_{31,\mathrm{f}}$ can be calculated by the following equation (Chun, Sato, and Kanno 2013).

$$e_{31,\mathrm{f}} = \frac{d_{31}}{s_{11}^p + s_{12}^p} \cong -\frac{h_s^2 E_s}{3(1-\nu_s)L^2} \cdot \frac{\delta}{V} \tag{1}$$

where d_{31} is the transverse piezoelectric constant, s_{11}, s_{12} are components of elastic compliance, h is the thickness, E is Young's modulus, ν is Poisson's ratio, L is the beam length, and V is the applied voltage. The superscript p and subscript s represent the piezoelectric thin films and substrates, respectively. Figure 3 shows the tip displacement and piezoelectric coefficient $e_{31,f}$ as functions of applied voltage. The tip displacement proportionally increased with applied voltage. The piezoelectric coefficient $e_{31,\ f}$ was almost constant at −4.8 C/m^2, a typical value of epitaxial PZT thin films on Pt/MgO substrates (Morimoto et al. 2010).

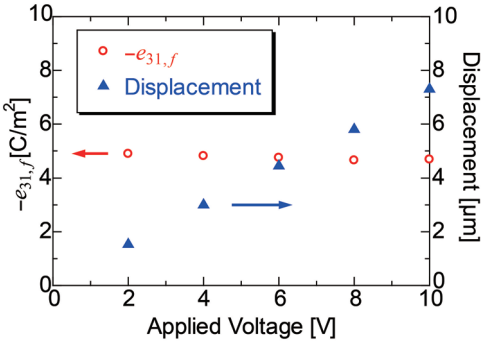

Figure 3: Tip displacement and piezoelectric coefficient of the unimorph cantilever of the transferred PZT thin film on a stainless steel cantilever as a function of applied voltage.

We evaluated the crystal structure of the transferred PZT thin films by X-ray diffraction (XRD). Figure 4 shows XRD patterns of the PZT thin films before and after transfer. The transferred PZT thin films exhibited strong *c*-axis orientation. These results indicate that LLO did not degrade the crystal structure of the film, allowing the PZT thin films to be transferred to a variety of materials without chemical etching.

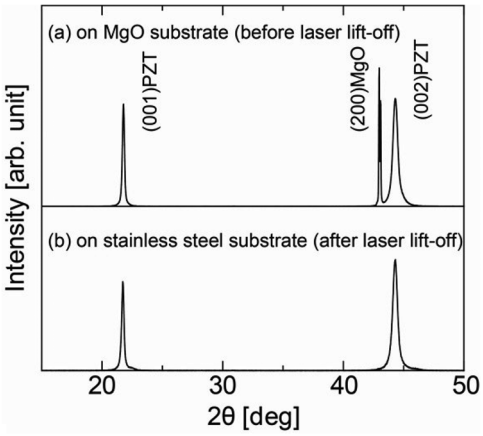

Figure 4: XRD patterns of PZT thin films: (a) PZT thin film on MgO substrate (before LLO) and (b) transferred PZT thin film (after LLO).

Power-generation performance

Figure 5 shows a schematic of the system used to measure the power-generation performance of the PVEHs. We mounted the PVEHs on a vibration exciter and measured the output voltage using a frequency response analyzer (FRA). To measure the vibrational acceleration of the PVEHs, we attached an acceleration pickup to the base of the cantilever.

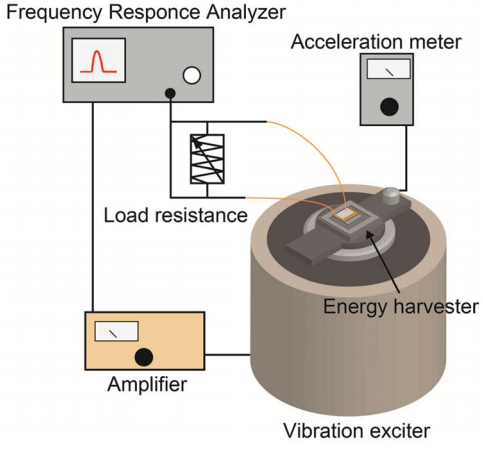

Figure 5: Schematic of measurement system for PVEHs.

First, we evaluated the frequency response of the output voltage and determined the resonance frequency by sweeping the excitation frequency in an open-circuit state at an acceleration of 1.0 m/s^2. Simultaneously, we measured the cantilever displacement by a laser Doppler vibrometer. To avoid errors caused by the large deflection of the tip in this measurement, we measured the displacement at 5 mm from the fixed end.

Figure 6 shows the frequency response of the output voltage and the cantilever displacement at an acceleration of 1.0 m/s^2. The voltage and displacement curves had similar shapes, and their peaks both appeared at 143 Hz, where the maximum voltage reached 2.5 $V_{p\text{-}p}$. Using the half-power bandwidth method, we obtained the quality factor (Q) from the resonance curves of displacement and output voltage to be 157.

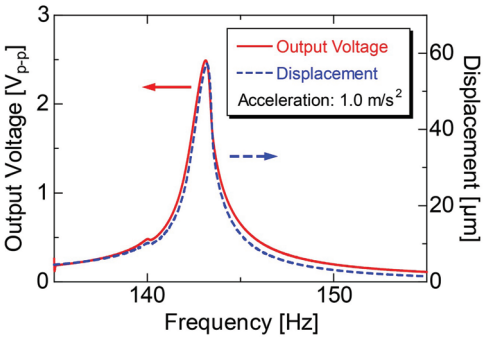

Figure 6: Output voltage in an open-circuit state and cantilever displacement at 5 mm from the fixed end as functions of frequency.

Although we measured the resonant frequency of the raw SS304 cantilever to be 115 Hz at an acceleration of 1.0 m/s^2, the PVEH exhibited higher resonance frequency (143 Hz) after transferring the PZT thin films. We attribute this increase to an increase in stiffness of the cantilever from the PZT/epoxy layers.

We then evaluated how the effective electric power depended on the parallel-connected load resistance at the resonance frequency under an acceleration of 1.0 m/s^2. We calculated effective electric power from the following equation.

$$P = \frac{V_{p-p}^2}{8R} \tag{2}$$

where P is the effective electric power, V_{p-p} is the peak-to-peak output voltage, and R is the load resistance. Figure 7 shows the output power and output voltage as

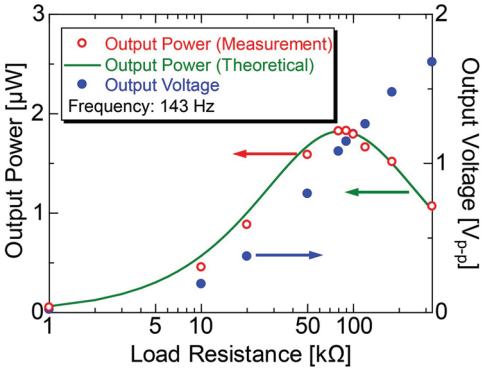

Figure 7: Output power and output voltage as functions of load resistance. The oscillation frequency and acceleration were 143 Hz and 1.0 m/s^2, respectively.

functions of load resistance. The maximum output power of 1.8 μW was obtained at a load resistance of 90 kΩ.

We evaluated the power-generation characteristics of the PVEHs using theoretical equations. The theoretical output power is expressed by the following equation (Renaud et al. 2008).

$$P = \frac{ma^2}{2\omega_0} \cdot \frac{K^2Q^2(\omega_0 RC)}{(\omega_0 RC)^2 + [1 + K^2Q(\omega_0 RC)]^2} \quad (3)$$

where m is the tip mass, a is the acceleration of the tip mass, ω_0 is the resonance frequency, K^2 is the generalized electromechanical coupling coefficient, Q is the quality factor, R is the load resistance, and C is the capacitance. Here, the optimal resistance R_{opt} to maximize P is expressed by the following equation.

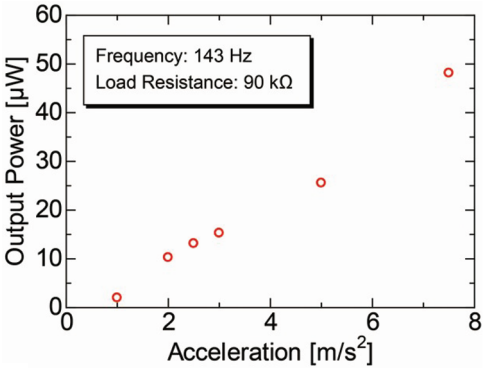

Figure 8: Output power as a function of acceleration. The oscillation frequency and load resistance were 143 Hz and 90 kΩ, respectively.

$$R_{opt} = \frac{1}{\omega_0 C\sqrt{1 + K^4Q^2}} \quad (4)$$

As described above, we calculated Q to be 157 at an acceleration of 1.0 m/s^2. Then we calculated the fitting K^2, back-calculated from eq. (3) using the measured output power. The fitting K^2 was calculated to be 3.28×10^{-3}. From eq. (3), we calculated the theoretical optimal load resistance and maximum effective output power at an acceleration of 1.0 m/s^2 to be 83 kΩ and 1.8 μW, respectively. These values agree well with the measured values, as shown in Figure 7. This result supports the validity of the experimentally measured optimal resistance and effective output power.

Figure 8 shows how the effective electric power depended on acceleration. As the acceleration increased, the output power increased to a maximum of 49 μW at an acceleration of 7.5 m/s^2. Although the output power theoretically increases with the square of acceleration, the experimental output power increased proportionally. In the previous study, we have observed that the Q of metal-based PVEHs rapidly decreased with the increase of acceleration (Tsujiura, Adachi, and Kanno 2012), and experimental output power was in good agreement with the calculated value if we took into account of the variation of Q. Therefore, proportional increase of output power of this study is also attributed to the decrease of Q with the acceleration.

Table 2 compares the performance of our PVEH with those from other studies. The normalized power density (NPD) is defined as the effective output power divided by the volume of the PVEH (volume of the cantilever) and the square of gravitational acceleration (Janphuang

Table 2: Comparison of the PVEH performance. The acceleration g is gravitational acceleration; 1 g equals 9.8 m/s^2.

Study	Piezoelectric material	Substrate	Active area [cm^2]	Active volume [cm^3]	Resonance Frequency [Hz]	Acceleration [g]	Output Power [μW]	Power density [μW/cm^2]	Normalized power density [μW/cm^{3}g^2]
Fang et al. (2006)	PZT thin films	Si	0.012	0.00078	608	1	2.16	180	2,769
Shen et al. (2008)	PZT thin films	Si	0.026	0.00066	461.15	2	2.15	84	814
Tsujiura, Adachi, and Kanno (2012)	PZT thin films	SS430	0.375	0.00392	365	1	6.8	18	1,735
Aktakka, Peterson, and Najafi (2011)	Thinned bulk PZT	Si	0.49	0.027	167	0.1	2.74	5.6	10,148
Janphuang et al. (2014)	Thinned bulk PZT	Si	1.242	0.04782	99.9	0.1	82.4	66	3,346
This study	Epitaxial PZT thin films	SS304	0.011*	0.0171**	143	0.1	1.8	159	10,526

Note: *Capacitive area.
**Volume of the cantilever.

et al. 2014). Note that the NPD values in Table 2 were calculated from the data of the references. The NPD of our PVEH exceeds those of PVEHs using non-epitaxial PZT thin films and is comparable to that of PVEHs using thinned bulk PZT. Transfer by LLO did not cause degradation, unlike wet etching, allowing us to use high-quality PZT thin films to fabricate PVEHs with high power-generation efficiency. Furthermore, thin SS304 cantilevers with built-in tip mass lowered the resonance frequency of the PVEH in spite of their small sizes. These results lead the way to high-efficiency microgenerators composed of epitaxial PZT thin films on flexible metal substrates.

Conclusions

In this study, we fabricated PVEHs of *c*-axis-oriented epitaxial PZT thin films. The epitaxial PZT thin films were deposited on MgO substrates by rf magnetron sputtering and were transferred to microfabricated SS304 cantilevers using LLO. The transferred epitaxial PZT thin films exhibited excellent piezoelectric properties, and we found no degradation caused by LLO transfer. At an acceleration of 1.0 m/s^2, the PVEHs exhibited a resonance frequency and generated output power of 143 Hz and 1.8 μW, respectively, and the output power reached a maximum of 49 μW at 7.5 m/s^2.

Compared with MEMS PVEHs composed of non-epitaxial films on Si cantilevers, our PVEH had higher volumetric power-generation efficiency and lower resonance frequency. From these results, we conclude that LLO is a promising means of transferring epitaxial PZT thin films to fabricate high-efficiency microgenerators.

References

Aktakka, E. E., R. L. Peterson, and K. Najafi. 2011. "Thinned-PZT on SOI Process and Design for Piezoelectric Internal Energy Harvesting." In *Proceedings of Transducers'11 Conference*: 1649–52.

Cao, Z., J. Zhang, and H. Kuwano. 2012. "Design and Characterization of Miniature Piezoelectric Generators with Low Resonant Frequency." *Sensors and Actuators A: Physical* 179:179–84.

Chun, D. M., M. Sato, and I. Kanno. 2013. "Precise Measurement of Transverse Piezoelectric Coefficient for Thin Films on Anisotropic Substrate." *Journal of Applied Physics* 113 (4):044111.

Do, Y. H., W. S. Jung, M. G. Kang, C. Y. Kang, and S. J. Yoon. 2013. "Preparation on Transparent Flexible Piezoelectric Energy Harvester Based on PZT Films by Laser Lift-Off Process." *Sensors and Actuators A: Physical* 200:51–5.

Do, Y. H., M. G. Kang, J. S. Kim, C. Y. Kang, and S. J. Yoon. 2012. "Fabrication of Flexible Device Based on PAN-PZT Thin Films by Laser Lift-Off Process." *Sensors and Actuators A: Physical* 108:124–7.

Ericson, F., S. Johansson, and J. A. Schweitz. 1988. "Hardness and Fracture Toughness of Semiconducting Materials Studied by Indention and Erosion Techniques." *Materials Science and Engineering: A* 105:131–41.

Fang, H. B., J. Q. Liu, Z. Y. Xu, L. Dong, L. Wang, D. Chen, B. C. Cai, and Y. Liu. 2006. "Fabrication and Performance of MEMS-Based Piezoelectric Power Generator for Vibration Energy Harvesting." *Microelectronics Journal* 37(11):1280–4.

Isarakorn, D., A. Sambri, P. Jamphuang, D. Briand, S. Gariglio, J. M. Triscone, F. Guy, J. W. Reiner, C. H. Ahn, and N. F. de Rooij. 2010. "Epitaxial Piezoelectric MEMS on Silicon." *Journal of Micromechanics and Microengineering* 20(5):055008.

Janphuang, P., R. Lockhart, N. Uffer, D. Briand, and N. F. de Rooij. 2014. "Vibrational Piezoelectric Energy Harvesters Based on Thinned Bulk PZT Sheets Fabricated at the Wafer Level." *Sensors and Actuators A: Physical* 210:1–9.

Kanda, K., I. Kanno, H. Kotera, and K. Wasa. 2009. "Simple Fabrication of Metal-Based Piezoelectric MEMS by Direct Deposition of Pb(Zr, Ti)O_3 Thin Films on Titanium Substrates." *Journal of Microelectromechanical Systems* 18(3):610–15.

Kanno, I., S. Fujii, and R. Takayama. 1997. "Piezoelectric Properties of c-Axis Oriented Pb(Zr, Ti)O_3 Thin Films." *Applied Physics Letters* 70(11):378–1380.

Kim, S. G., S. Priya, and I. Kanno. 2012. "Piezoelectric MEMS for Energy Harvesting." *MRS Bulletin* 37(11):1039–50.

Lee, C. H., S. J. Kim, Y. Oh, M. Y. Kim, Y. J. Yoon, and H. S. Lee. 2010. "Use of Laser Lift-Off for Flexible Device Applications." *Journal of Applied Physics* 108(10):102814.

Lin, S. C., and W. J. Wu. 2013. "Piezoelectric Micro Energy Harvesters Based on Stainless Steel Substrates." *Smart Materials and Structures* 22(4):045016.

Morimoto, K., I. Kanno, K. Wasa, and H. Kotera. 2010. "High-Efficiency Piezoelectric Energy Harvesters of c-Axis-Oriented Epitaxial PZT Films Transferred Onto Stainless Steel Cantilevers." *Sensors and Actuators A: Physical* 163(1):428–32.

Murase, S., S. Kobatake, M. Tanaka, I. Tashiro, O. Horigami, H. Ogiwara, K. Shibata, K. Nagai, and K. Ishibashi. 1993. "Effects of a High Magnetic Field on Fracture Toughness at 4.2 K for Austenitic Stainless Steels." *Fusion Engineering and Design* 20:451–4.

Pandey, P. K., A. R. James, R. Raman, S. N. Chatterjee, A. Goyal, C. Prakash, and T. C. Goel. 2005. "Structural, Ferroelectric and Optical Properties of PZT Thin Films." *Physica B* 369(1–4): 135–42.

Park, K., J. H. Son, G. T. Hwang, C. K. Jeong, J. Ryu, M. Koo, I. Choi, S. H. Lee, M. Byun, Z. L. Wang, et al. 2014. "Highly-Efficient, Flexible Piezoelectric PZT Thin Film Nanogenerator on Plastic Substrates." *Advanced Materials* 26(16):2514–20.

Renaud, M., K. Karakaya, T. Sterken, P. Fiorini, C. Van Hoof, and R. Puers. 2008. "Fabrication, Modelling and Characterization of MEMS Piezoelectric Vibration Harvesters." *Sensors and Actuators A: Physical* 145:380–6.

Shen, D., J. H. Park, J. Ajitsaria, S. Y. Choe, C. I. I. I. Haward, and D. J. Kim. 2008. "The Design, Fabrication and Evaluation of a MEMS

PZT Cantilever with an Integrated Si Proof Mass for Vibration Energy Harvesting." *Journal of Micromechanics and Microengineering* 18(5):055017.

Tomioka, K., F. Kurokawa, R. Yokokawa, H. Kotera, K. Adachi, and I. Kanno. 2012. "Composition Dependence of Piezoelectric Properties of Pb(Zr, Ti)O_3 Films Prepared by Combinatorial Sputtering." *Japanese Journal of Applied Physics* 51(9):09LA12.

Trolier-Mckinstry, S., and P. Muralt. 2004. "Thin Film Piezoelectrics for MEMS." *Journal of Electroceramics* 12(1–2):7–17.

Tsakalakos, L., and T. Sands. 2000. "Epitaxial Ferroelectric (Pb,La)(Zr,Ti)O_3 Thin Films on Stainless Steel by Excimer Laser Liftoff." *Applied Physics Letters* 76(2):227–9.

Tsakalalos, L., T. Sands, E. Carleton, and K. M. Yu. 2003. "Modification of (Pb,La)(Zr,Ti)O_3 Thin Films During Pulsed Laser Liftoff From MgO Substrates." *Journal of Applied Physics* 94(6):4047–52.

Tsujiura, Y., K. Adachi, and I. Kanno. 2012. "Piezoelectric MEMS Energy Harvesters of PZT Thin Films on Stainless Steel Cantilevers." In *Proceedings of PowerMEMS'12 Conference*: 500.

Tsujiura, Y., E. Suwa, F. Kurokawa, H. Hida, K. Suenaga, K. Shibata, and I. Kanno. 2013. "Lead-Free Piezoelectric MEMS Energy Harvesters of (K, Na)O_3 Thin Films on Stainless Steel Cantilevers." *Japanese Journal of Applied Physics* 52(9):09KD13.

Yeager, C. B., and S. Trolier-McKinstry. 2012. "Epitaxial Pb(Zr_x,Ti_{1-x})O_3 ($0.30 \leqslant x \leqslant 0.63$) Films on (100)MgO Substrates for Energy Harvesting Applications." *Journal of Applied Physics* 112(7):074107.

Yin, S., G. Niu, B. Vilquin, B. Gautier, G. Le Rhun, E. Defay, and Y. Robach. 2012. "Epitaxial Growth and Electrical Measurement of Single Crystalline Pb($Zr_{0.52}$ $Ti_{0.58}$)O_3 Thin Film on Si(001) for Micro-Electromechanical Systems." *Thin Solid Films* 520(14):4572–5.

Yokoyama, S., Y. Honda, H. Morioka, S. Okamoto, and H. Funakubo. 2005. "Dependence of Electrical Properties of Epitaxial Pb(Zr, Ti)O_3 Thick Films on Crystal Orientation and Zr/(Zr + Ti) Ratio." *Journal of Applied Physics* 98(9):09416.